Journal of Materials Chemistry B

Accepted Manuscript

This is an *Accepted Manuscript*, which has been through the Royal Society of Chemistry peer review process and has been accepted for publication.

Accepted Manuscripts are published online shortly after acceptance, before technical editing, formatting and proof reading. Using this free service, authors can make their results available to the community, in citable form, before we publish the edited article. We will replace this *Accepted Manuscript* with the edited and formatted *Advance Article* as soon as it is available.

You can find more information about *Accepted Manuscripts* in the Information for Authors.

Please note that technical editing may introduce minor changes to the text and/or graphics, which may alter content. The journal's standard Terms & Conditions and the Ethical guidelines still apply. In no event shall the Royal Society of Chemistry be held responsible for any errors or omissions in this *Accepted Manuscript* or any consequences arising from the use of any information it contains.

ROYAL SOCIETY OF CHEMISTRY

www.rsc.org/materialsB

One-step synthesis of biocompatible magnetite/silk fibroin core shell nanoparticles

Weiqin Sheng, ‡[a] Jing Liu, ‡[b] Shanshan Liu,[a] Qiang Lu, *[a] David L Kaplan,[a c] Hesun Zhu[d]

[a]*National Engineering Laboratory for Modern Silk & Collaborative Innovation Center of Suzhou Nano Science and Technology, Soochow University, Suzhou 215123, People's Republic of China. Tel: (+86)-512-67061649; E-mail: Lvqiang78@suda.edu.cn*

[b]*Regenerative Medicine Center, First Affiliated Hospital of Dalian Medical University, No.222 Zhongshan Road, Dalian 116011, People's Republic of China*

[c]*Department of Biomedical Engineering, Tufts University, Medford, MA 02155, USA*

[d]*Research Center of Materials Science, Beijing Institute of Technology, Beijing, 100081, People's Republic of China*

‡ These authors contributed equally to this work.

Journal of Materials Chemistry B Accepted Manuscript

TOC

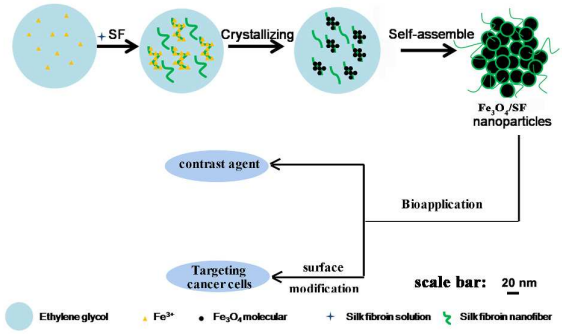

Core-shell Fe_3O_4/SF nanoparticles, prepared by silk fibroin with one step, could be widely used in biomedical areas, such as contrast agent and targets with some surface modification.

Journal of Materials Chemistry B Accepted Manuscript

Cite this: DOI: 10.1039/c0xx00000x

www.rsc.org/xxxxxx

ARTICLE TYPE

One-step synthesis of biocompatible magnetite/silk fibroin core-shell nanoparticles

Weiqin Sheng, ‡ [a] Jing Liu,‡ [b] Shanshan Liu[a], Qiang Lu,* [a] David L Kaplan,[a c] and Hesun Zhu[d]

Received (in XXX, XXX) Xth XXXXXXXXX 20XX, Accepted Xth XXXXXXXXX 20XX
DOI: 10.1039/b000000x

A one-step hydrothermal process with silk fibroin (SF) nanofiber as template and coating was developed to synthesize core-shell magnetite/SF nanoparticles with limited controllable sizes. The Fe_3O_4 nanoparticles gradually aggregated into nanospheres with increased sizes from 120 to 500 nm by increasing the SF content in the reaction system. The magnetic properties and biocompatibility of Fe_3O_4/SF nanoparticles, as well as their functional ability with antibody were also discussed to assess their possible applications in MRI and bio-separation. Compared to previous two-step process, our one-step method provides a simpler and more cost-effective approach to preparing biocompatible core-shell magnetite nanoparticles.

Keywords: Fe_3O_4, silk, core-shell nanoparticles, biocompatibility, Magnetic resonance imaging (MRI)

Introduction

There is an urgent requirement to develop multifunctional nanocomposites that could combine sensing, diagnostic and therapeutic functions within a single nanostructure.[1-10] Among these nanocomposites, superparamagnetic iron oxide nanoparticles with biocompatible shells are in great demand because of their low cost and environmentally benign nature, as well as their promising potential in drug delivery,[11-15] magnetic resonance imaging (MRI),[16-20] magnetic hyperthermia,[21- 23] tissue repair,[24-26] and bio-separation.[9, 27] In these applications, good dispersibility without scarify of biocompatibility is a prerequisite. Much effort has been devoted to the fabrication of core-shell superparamagnetic nanoparticles with uniform size and good dispersibility in aqueous solution.[1, 2] Magnetic microspheres with tailored functional polymer shell have attracted special attention. Both synthetic and natural polymers, such as PEG, [12, 28] chitosan, [19] alginate, [29, 30] dextran, [31] poly (vinylpyrrolidone) (PVP) [32] or poly (vinyl alcohol) (PVA), [33] have been used to stabilize Fe_3O_4 microspheres, offering long-term stability and biocompatibility. Different natural polymers are considered as preferred choice because of their better biocompatibility, nontoxicity and easy conjugation with various functional groups. Several synthetic or coating strategies have been developed to fabricate Fe_3O_4 microspheres with natural polymers as the shell. However, tedious preparation steps remain main challenges of their wide applications. Simple and effective processes are urgently needed for core-shell magnetic microsphere formation.

B mori SF, a naturally derived polymer, has been utilized in various technological fields including tissue regeneration, [36] drug release, [37, 38] optical components and electronic applications [39-42]. Its nanostructures and hydrophobic/hydrophilic properties can be

Journal of Materials Chemistry B Accepted Manuscript

regulated through controlling its self-assembly process, providing promising templates for different functional nanoparticles such as copper oxide, [43] silver [44] and others. [35, 45] Several cost-effective methods have been developed to prepare silk nanoparticles in aqueous solution, which further offered different templates for these applications.[19,30,34,35] Although a few studies have reported the fabrication of SF-coated magnetic nanoparticles,[35, 46] the success in achieving satisfactory water-dispersibility for these nanoparticles has been limited. Huang group[46] fabricated Fe_3O_4/SF nanoparticles with irregular structures. However, further improvement is still required to control the morphology for biomedical applications such as drug release. Chen group[35] achieved the morphology control using SF as template. Unfortunately, they could only prepare Fe_2O_3/SF nanoparticles whose magnetism is not strong enough for bio-separation and MRI applications. In our study, more SF was added in the Fe_3O_4 reaction system to achieve Fe_3O_4/SF nanoparticles with regular morphology and stronger magnetism, providing better candidate for bio-separation, MRI and drug release applications.

Overall, we developed a one-step solvothermal process to synthesize core-shell Fe_3O_4/SF nanomaterial with homogeneous size and water-dispersibility. Our results suggested that SF could be used to control the morphology and size of Fe_3O_4 microspheres. The biocompatibility and transverse relaxivity (typical characterization of the MRI efficiency) of the Fe_3O_4/SF core-shell nanomaterial, as well as their easily coupling ability with antibody, suggest their future applications in different biomedical applications.

Experimental Section

Materials

Iron chloride hexahydrate ($FeCl_3 \cdot 6H_2O$), Sodium acetate trihydrate ($NaAc \cdot 3H_2O$), Ethylene glycol (EG), Ethanol and Na_2CO_3 were purchased from Sinopharm Chemical Reagent Co., Ltd., Shanghai, China. LiBr was bought from Sigma-Aldrich. All the reagents were used without further purification.

Preparation of SF solutions

SF solutions were prepared according to our previously published procedures.[47] *B mori* cocoons were boiled for 20 min in an aqueous solution of 0.02 M Na_2CO_3 and then rinsed thoroughly with distilled water to extract the sericin proteins. After drying, the extracted silk was dissolved in 9.3M LiBr solution at 60°C for 4 h, yielding a 20% (w/v) solution. This solution was dialyzed against distilled water using dialysis tube (MWCO 3500) for 72 h to remove the salt. Then the solution was centrifuged at 9000 rpm for 20 min at 4 °C to remove silk aggregations formed during the process. The final concentration of SF in water was about 7 wt%, determined by weighing the remained solid after drying. The prepared SF solution was stored at 4 °C for future use.

Synthesis of Fe_3O_4/SF nanomaterial

Core shell Fe_3O_4/SF nanoparticles were synthesized with a modified solvothermal procedure.[48] In a typical procedure, 1.35g iron chloride hexahydrate ($FeCl_3 \cdot 6H_2O$) and 5.97g $NaAc \cdot 3H_2O$ were dissolved in 60ml ethylene glycol (EG) under stirring for 0.5 h. Then 10ml of 7 wt% SF solution was added into the blend under continuous stirring for another 0.5 h to form transparent solution. The solution was transferred into a 100ml Teflon-lined stainless-steel autoclave. After maintained at 160 °C for 12 h, the autoclave was cooled at room temperature. The as-prepared Fe_3O_4/SF nanoparticles were collected and separated from free SF by centrifuging the solution at 8000 rpm for 30 min, and then washed by ethanol and water for three times, respectively. 10 ml of SF solution with different concentrations were also added into the above reaction system to achieve Fe_3O_4/SF nanoparticles with various morphologies and sizes.

Journal of Materials Chemistry B Accepted Manuscript

This journal is © The Royal Society of Chemistry [year]

Characterizations

X-ray diffraction (XRD) patterns of the samples were recorded on a X'Pert-Pro diffractometer (PANalytical, Holland) with Cu Kα radiation in the 2θ range from 10 to 90° at 40 kV and 40 mA. The hydrodynamic diameter and zeta potential of Fe_3O_4/SF were determined with a Malvern Zetasizer Nano ZS90 instrument. The magnetic properties of the products were characterized by vibrating sample magnetometry (VSM) in an applied magnetic field sweeping from -20 KOe to 20 KOe at 300 K. The phase of Fe_3O_4/SF was determined by Tecnai FEI 20 transmission electron microscopy (TEM). SEM images were obtained with a field emission scan electron microscopy (SEM, SU8010, Hitachi, Japan) at 15kV. Additionally, the inductively coupled plasma atomic emission spectroscopy (ICP-AES, OPTIMA 8000, PerkinElmer, USA) was used to analyze the element of Fe in the samples. During this process, Fe solution with standard concentration (5 ppm, 25 ppm, 50 ppm) was used to determine a calibration curve.

Cellular experiment

Human dermal fibroblasts (Hs 865.Sk cell, American Type Culture Collection, ATCC) and human lung cancer cells (NCI-H460 cells, Cell Bank of Chinese Academy of Sciences, Shanghai, China) were cultured with Fe_3O_4/SF nanoparticles to assess the influence of the nanoparticles on normal and cancel cells, respectively.

Hs 865.Sk cells were cultured in Dulbecco's Modified Eagle's Medium (DMEM medium) supplemented with 10% fetal bovine serum (FBS) and 1% IU ml^{-1} streptomycin-penicillin (all from Invitrogen, Carlsbad, CA). NCI-H460 cells were grown in RPMI-1640 culture medium supplemented with 10% fetal bovine serum (FBS) and 1% streptomycin-penicillin. All the cells were maintained in a humidified incubator containing 5% CO_2 at 37 °C.

CCK-8 assay is an effective way of determining the number of viable cells.[49] Considering it could provide more sensitive results than that of MTT, XTT, MTS or WST-1 assays, the CCK-8 assay was used to assess the cytotoxicity of Fe_3O_4/SF and pure Fe_3O_4 samples. Typically, 100 μ L of cells (1×10^4 cells per well) were seeded in 96-well plates and incubated for 24h. Then, Fe_3O_4/SF with different concentrations (the equivalent Fe concentrations were 100, 80, 60, 40, 20, 10 and 0 μg Fe/ml) were added into each group and incubated for another 24h. After discarding the culture medium, the cells were treated with 10% CCK8 in MPC media (no phenol red) for 1 h at 37 °C. Absorbance at 450 nm was measured using a microplate reader (Bio-Tek synergy 4, BioTek, USA). Cell viability in eight parallel wells was evaluated for each dose above, and each experiment was repeated at least three times. Cell viability was calculated by means of the following formula:

$$\text{Cell viability}\ (\%) = \frac{\text{OD450(sample)} - \text{OD450(blank)}}{\text{OD450(control)} - \text{OD450(blank)}} * 100\%$$

FITC-Avidin was used to couple with Fe_3O_4/SF nanoparticles to assess the possibility of specific cancer cell targeting ability. Typically, FITC-Avidin was firstly used to couple with Fe_3O_4/SF nanoparticles by EDC coupling reaction. Then, 200 μL of the stock solution (biotinylated anti-CD3 antibody was dissolved in PBS buffer to make a 0.5 mg /ml stock solution) was mixed with 250 μL of FITC-Avidin-coupled Fe_3O_4/SF nanoparticles suspension. The mixture was incubated for 20 min at room temperature and then centrifuged at 10000 rpm for 5 min. The obtained nanoparticles were washed two more times with 1 ml PBS buffer each time. Lastly, 2 ml of cell suspension (2×10^5 cells /ml) was added to each well of a 12-well plate and incubated with 200 μg of Biotinylated anti-CD_3 antibody-FITC-Avidin-Fe_3O_4/SF. The plate was incubated at 37 °C for 2 h, and then the cells were spun down at 1000 rpm for 10 min and re-suspended in PBS

Journal of Materials Chemistry B Accepted Manuscript

buffer. The cells were imaged using a confocal laser scanning microscope (AXIO OBSERVER A1, Zeiss, Germany).[50]

Measurement of T_2 relaxivity

T_2 relaxivity means the efficiency of spin-spin relaxation. Stronger T_2 relaxivity leads to more obvious decrease in signal intensity of various target organs on T_2-weighted images.[51, 52] In order to measure the T_2 relaxivity, Fe_3O_4/SF nanoparticles and Fe_3O_4 nanoparticles with different iron concentrations were dispersed in 1% agarose solution. The samples were scanned at room temperature using a T_2-weighted fast spin-echo multi-slice sequence (fSEMS) (TR/TE=3,000/13.6, 27.2, 54.4, 81.6, 136 ms, slice thickness=2.0 mm) by a 3T MRI scanner (3T Trio Tim, Siemens).[16]

Statistical analysis

Statistical analysis was conducted using the two-tailed Student's test. The data were presented as means ± S.D. obtained from three independent experiments. Results were considered to be statistically significant at $P<0.05$.

Results and discussion

The superparamagnetic nanoparticles used in biomedical applications need to be coated with biocompatible polymers for its long-term stability and further functionalization. At least two steps including Fe_3O_4 nanoparticle formation and then coating process are generally required to form the final core shell structure. A one-step approach was developed to prepare superparamagnetic nanoparticles with SF as template and coating material in our present study, providing a simpler and more feasible way for core-shell Fe_3O_4/SF nanoparticle fabrication.

Figure 1 showed the SEM images of Fe_3O_4 nanoparticles prepared with different amounts of SF as template and coating material. The formed pure Fe_3O_4 nanoparticles showed irregular morphologies with size of about 20 nm. Following the increase of SF in the reaction system, the Fe_3O_4 nanoparticles became more regular and finally transformed into nanospheres when the concentration of SF was above 7%. The size of the Fe_3O_4 nanospheres could be further increased from 120 nm to 200 nm and 500 nm if the SF concentration was 10 % and 15 %, respectively, which was consistent with the dynamic light scattering results (Figure S1 in the supporting information, SI). The size distribution of the Fe_3O_4/SF particles was also supplied in Figure S1. Although the diameters of the nanoparticles increased following the increase of SF concentration, more Fe_3O_4/SF particles with inhomogeneous diameters appeared when the SF concentrations were 10 wt% and 15 wt%. The results indicated that best morphology control of the nanoparticles was achieved when the SF concentration was 7 wt%. The high-magnification SEM image (Figure S2) indicated that these nanospheres were composed of smaller nanoparticles (10 nm). Transmission electron microscopy (TEM) provided further insight into the morphology and microstructure of the different nanoparticles (Figure 2). The same morphology transition from irregular shape to nanospheres also appeared in TEM images, which was consistent with the SEM observations. Some pale areas and dark smaller nanoparticles were also observed inside Fe_3O_4 nanospheres, indicating that the nanospheres were not totally compact and aggregated from smaller Fe_3O_4 particles. In addition, it also can be observed that the surface of nanospheres became blurry because of SF coating. Zeta potential changes of our products also confirmed the formation of SF coating outside the nanospheres. The compact SF coating could gradually form and result in maximum negative value of zeta potential when the SF concentration increased from 0 to 7 wt%. After the SF concentration further increased, the thickness of the compact SF

Journal of Materials Chemistry B Accepted Manuscript

This journal is © The Royal Society of Chemistry [year]

coating increased while the zeta potential became more positive, possibly due to the aggregation of SF in the reaction process.[53]Although further study is still necessary to clarify the reason for the zeta potential change of the different Fe_3O_4 nanospheres, the TEM and zeta potential results had confirmed that SF could be coated on the Fe_3O_4 particles to form core-shell structure through simple one-step process. Furthermore, SF coating formed outside the nanoparticles was uniform due to the strong coordinative effect of –COO-Fe.[54-57] The coating thickness slightly increased from 2.7 nm to 4.4 and 5.3 nm when the SF concentrations were 7 wt%, 10 wt% and 15 wt%, respectively.

The desired Fe_3O_4 phase formation was evaluated with X-ray powder diffraction (XRD). Figure 3 showed the XRD patterns of Fe_3O_4 and Fe_3O_4/SF nanoparticles. Six diffraction peaks appeared at 2θ = 30.3°, 35.6°, 43.3°, 53.7°, 56.9° and 62.9°, which correspond to the (220), (311), (400), (422), (511) and (440) planes of Fe_3O_4 (JCPDS card no. 01-089-2355), respectively. No evident differences were observed for pure Fe_3O_4 and Fe_3O_4/SF nanoparticles, suggesting that the crystalline structure of the nanoparticles was not affected by SF coating. Following the increase of SF content in the reaction system, the intensities of the Fe_3O_4 diffraction planes in the Fe_3O_4/SF nanoparticles increased and finally achieved a platform when the SF concentration was above 7%. These results implied that suitable amount of SF could promote the crystallization of Fe_3O_4 in the reaction system.

Several studies have revealed that SF can induce crystallization and formation of Fe_3O_4 nanoparticles.[46, 58-60] However, the morphology control of the Fe_3O_4/SF nanoparticles remains a challenge. It is generally believed that the tyrosine residues in SF macromolecular chains have a strong interaction with Fe (III), [61-62] making silk-Fe complexes possible in different reaction systems. More recently, Chen et al prepared hematite nanoparticles by a SF-assisted hydrothermal method.[35] They further clarified the multiple functions of SF in Fe_2O_3 formation process. SF chains firstly induced spherical Fe_2O_3 nanoparticle formation and then controlled further growth to achieve primary nanoparticles. Afterword, the self-assemble of SF chains on the surface of those primary nanoparticles led to the formation of large nanospheres. Although Fe_3O_4 nanospheres were not synthesized by a similar SF-assisted hydrothermal method in their group and the shape of Fe_2O_3 nanospheres was not round, the study implied that the ratios, secondary conformations and nanostructures of SF in the reaction system were critical in the morphology control of the different nanoparticles. Therefore, different to previous SF-assisted hydrothermal method, SF was firstly assembled into nanofibers with higher zeta potential (-33.1 mV) along with the addition of EG in our study (Figure S3), providing stronger interaction with Fe (III) and also stronger aggregations of the primary nanoparticles. After the modification, Fe_3O_4/SF core-shell nanospheres with improved round shapes and bigger sizes were achieved through similar hydrothermal process (Scheme 1). The fabrication of magnetic nanoparticles with biocompatible and biodegradable shells has been developed in recent years. Natural biomaterials such as chitosan and alginate have been used to coat the Fe_3O_4 nanoparticles.[19, 30] However, the preparation of Fe_3O_4 nanoparticles and the coating formation were different processes in the previous studies, resulting in at least two steps for the core-shell nanoparticles. In our study, the core-shell nanospheres with limited controllable sizes were easily prepared in a one-step process, which would facilitate further biomedical applications and modifications.

The Fe_3O_4/SF nanoparticles prepared form the reaction system containing 7wt% SF were then used to assess its possible biomedical applications since the formed nanoparticles had more uniform morphology, and better dispersibility in aqueous

Journal of Materials Chemistry B Accepted Manuscript

solution. The magnetism of Fe_3O_4/SF and Fe_3O_4 nanoparticles were measured by sweeping the external magnetic field between -20 and 20 KOe at room temperature (Figure 4a). The Fe_3O_4/SF nanoparticles showed insignificant coercivity, suggesting the superparamagnetic nature of the particles. The saturation magnetization (M_s) of Fe_3O_4/SF nanoparticles was decreased to a value 35 emu/g, compared to 50 emu/g of the control (pure Fe_3O_4 nanoparticles), which could be ascribed to the weight contribution from SF coating. TGA results further confirmed the assumption (Figure S4). Although the M_s was decreased after SF formation, it was still large enough to facilitate the quick separation of particles from solution, using a regular magnetic plate (Figure 4a insert).

The potential of Fe_3O_4/SF nanoparticles as a contrast agent was examined by using a 3T MR scanner. An obvious darkening of T_2-weighted MRI was observed with the increasing concentration of Fe, showing a transverse relaxivity (r_2) 40 $mM^{-1}s^{-1}$ (Figure 4). Although the value of transverse relaxivity is still inferior to some results reported in other works,[54, 55] a similar relaxivity with VSOP-C184 and Supravist was achieved in our Fe_3O_4/SF nanoparticles, which indicates the potential application of the Fe_3O_4/SF nanoparticles as MRI contrast agents.

The cytotoxicity of Fe_3O_4/SF and Fe_3O_4 nanoparticles was investigated with CCK8 assay. The Hs 865.Sk and NCI-H460 cells were incubated with Fe_3O_4/SF and Fe_3O_4 nanoparticles for 24h with concentrations of 10, 20, 40, 60, 80 and 100 μg Fe /ml (measured by ICP-AES) at 37 ^{o}C (Figure 5). The results showed that above 80% of cells maintained viable even at highest concentration of 100 μg Fe /ml, indicating the good biocompatibility of the core-shell Fe_3O_4/SF nanoparticles.

The surface area of the Fe_3O_4/SF nanoparticles was measured with nitrogen adsorption-desorption isotherms (Figure S5). The Brunauer-Emmett-Teller (BET) surface area of the Fe_3O_4/SF nanoparticles was 46 m^2g^{-1}, significantly higher than that of pure Fe_3O_4 nanoparticles (6 m^2g^{-1}). The results suggest a potential application of the Fe_3O_4/SF nanoparticles as a drug carrier. Then, FITC-Avidin that could bind Biotinylated anti-CD_3 antibody through Avidin-biotin interaction was used to couple with Fe_3O_4/SF nanoparticles, offering the Fe_3O_4/SF nanoparticles specific cancer cell targeting ability.[50] As shown in Figure 6, after incubation with the T-lymphocytic cell line Jurkat and human bone marrow-derived mesenchymal stem cell, stronger green fluorescence (Biotinylated anti-CD_3 antibody-FITC-Avidin-Fe_3O_4/SF) attaching to the cell was achieved in positive group, suggesting successful couple of Biotinylated anti-CD_3 antibody-FITC-Avidin with the nanoparticles.[50] The results indicated that the NPs prepared in our study could be further designed as targeting vehicle by surface modification, and then used to distinguish cancer cells from normal cells. However, it was also found that not all T-lymphocytes were labeled and the aggregation of nanoparticles appeared, which might be due to the neutralization of negative charge in the system. Coating the nanoparticless with polymers with positive charge through layer-by-layer process might be a feasible way to resolve the problem but makes the method more complicated, which should be further studied in our next work. Overall, the biocompatibility, magnetism, and higher surface area of the Fe_3O_4/SF nanoparticles imply their potential applications in MRI contrast agents and drug carriers.

Conclusions

Biocompatible core-shell Fe_3O_4/SF nanoparticles was successfully prepared via a one-step solvothermal process. Changing the contents of SF in reaction system could modulate the sizes of the nanoparticles in the range of 120-500 nm. The suitable magnetism, biocompatibility as well as further

Journal of Materials Chemistry B Accepted Manuscript

This journal is © The Royal Society of Chemistry [year]

fabrication ability of the nanoparticles implied their promising applications in different biomedical fields. Therefore, our present study provides a new way to design functional Fe_3O_4/SF nanoparticles.

Notes and references

[a]*National Engineering Laboratory for Modern Silk & Collaborative Innovation Center of Suzhou Nano Science and Technology, Soochow University, Suzhou 215123, People's Republic of China. Tel: (+86)-512-67061649; E-mail: Lvqiang78@suda.edu.cn.*

[b] *Regenerative Medicine Center, First Affiliated Hospital of Dalian Medical University, No.222 Zhongshan Road, Dalian 116011, People's Republic of China*

[c]*Department of Biomedical Engineering, Tufts University, Medford, MA 02155, USA*

[d]*Research Center of Materials Science, Beijing Institute of Technology, Beijing, 100081, People's Republic of China*

† Electronic Supplementary Information (ESI) available: [DLS and zeta potential of the products with different SF concentrations; high-magnification SEM of the products with 7% SF; AFM images of SF before and after addition of EG; TGA curves of the Fe_3O_4/SF and pure Fe_3O_4]. See DOI: 10.1039/b000000x/

‡ These authors contributed equally to this work.

1. J. E. Lee, N. Lee, T. Kim, J. Kim, and T. Hyeon, *Acc. Chem. Res.*, 2011, **44**, 893.
2. D. E. Lee, H. Koo, I. C. Sun, J. H. Ryu, K. Kim, and I. C. Kwon, *Chem. Soc. Rev.*, 2012, **41**, 2656.
3. J. Gao, H. Gu, and B. Xu, *Acc. Chem. Res.*, 2009, **42**, 1097.
4. Y. D. Jin, C. X. Jia, S. W. Huang, M. O'Donnell, and X. H. Gao, *Nat. Commun.*, 2010, **1**, 41.
5. S. H. Hu, and X. Gao, *J. Am. Chem. Soc.*, 2010, **132**, 7234.
6. Z. Y. Xiao, E. Levy-Nissenbaum, F. Alexis, A. Lupták, B. A. Teply, J. M. Chan, J. J. Shi, E. Digga, J. Cheng, R. Langer, and O. C. Farokhzad, *ACS Nano*, 2012, **6**, 696.
7. D. Kim, Y. Y. Jeong, and S. Jon, *ACS Nano*, 2010, **4**, 3689.
8. T. D. Schladt, M. I. Shukoor, K. Schneider, M. N. Tahir, F. Natalio, I. Ament, J. Becker, F. D. Jochum, S. Weber, O. Köhler, P. Theato, L. M. Schreiber, C. Sönnichsen, H. C. Schröder, W. E. G. Müller, and W. Tremel, *Angew. Chem. Int. Ed.*, 2010, **49**, 3976.
9. J. Wang, G. Z. Zhu, M. X. You, E. Song, M. I. Shukoor, K. J. Zhang, M. B. Altman, Y. Chen, Z. Zhu, C. Z. Huang, and W. H. Tan, *ACS Nano*, 2012, **6**, 5070.
10. J. F. Lovell, C. S. Jin, E. Huynh, H. Jin, C. Kim, J. L. Rubinstein, W. C. W. Chan, W. Cao, L. V. Wang, and G. Zheng, *Nat. Mater.*, 2011, **10**, 324.
11. M. I. Majeed, Q. W. Lu, W. Yan, Z. Li, I. Hussain, M. N. Tahir, W. Tremele, and B. Tan, *J. Mater. Chem. B*, 2013, **1**, 2874.
12. C. Wang, H. Xu, C. Liang, Y. M. Liu, Z. W. Li, G. B. Yang, L. Cheng, Y. G. Li, and Z. Liu, *ACS nano*, 2013, **7**, 6782.
13. Q. A. Pankhurst, J. Connolly, S. K. Jones, and J. Dobson, *J. Phys. D : Appl. Phys.*, 2003, **36**, R167.
14. J. Kim, J. E. Lee, J. Lee, J. H. Yu, B. C. Kim, K. An, Y. Hwang, C. H. Shin, J. G. Park, J. Kim, and T. Hyeon, *J. Am. Chem. Soc.*, 2006, **128**, 688.
15. B. Luo, S. Xu, A. Luo, W. R. Wang, S. L. Wang, J. Guo, Y. Lin, D. Y. Zhao, and C. C. Wang, *ACS nano*, 2011, **5**, 1428.
16. Z. H. Zhao, Z. J. Zhou, J. F. Bao, Z. Y. Wang, J. Hu, X. Q. Chi, K. Y. Ni, R. F. Wang, X. Y. Chen, Z. Chen, and J. H. Gao, *Nat. Commun.*, 2013, **4**, 2266.
17. H. X. Wu, S. J. Zhang, J. M. Zhang, G. Liu, J. L. Shi, L. X. Zhang, X. Z. Cui, M. L. Ruan, Q. J. He, and W. B. Bu, *Adv. Funct. Mater.*, 2011, **21**, 1850.
18. X. Y. Shi, S. H. Wang, S. D. Swanson, S. Ge, Z. Y. Cao, M. E. V. Antwerp, K. J. Landmark, and J. R. Baker. Jr, *Adv. Mater.*, 2008, **20**, 1671.

Journal of Materials Chemistry B Accepted Manuscript

19. J. L. Arias, L. H. Reddy, and P. Couvreur, *J. Mater. Chem.*, 2012, **22**, 7622.
20. P. Kucheryavy, J. B. He, V. T. John, P. Maharjan, L. Spinu, G. Z. Goloverda, and V. L. Kolesnichenko, *Langmuir*, 2013, **29**, 710.
21. X. J. Song, H. Gong, S. N. Yin, L. Cheng, C. Wang, Z. W. Li, Y. G. Li, X. Y. Wang, G. Liu, and Z. Liu, *Adv. Funct. Mater.*, 2014, **24**, 1194.
22. L. S. Lin, Z. X. Cong, J. B Cao, K. M. Ke, Q. L. Peng, J. H. Gao, H. H. Yang, G. Liu, and X. Y. Chen, *ACS Nano*, 2014, **8**, 3876.
23. Z. W. Li, S. N.Yin , L. Cheng , K. Yang , Y. G. Li , and Z. Liu, *Adv. Funct. Mater.*, 2014, **24**, 2312.
24. N. Tran, D. Hall, and T. J. Webster, *Nanotechnology*, 2012, **23**, 455104.
25. I. Bajpai, K. Balani, and B. Basu, *J. Am. Ceram. Soc.*, 2013, **96**, 2100.
26. W. Chen, T. Long, Y. J. Guo, Z. A. Zhu, and Y. P. Guo, *J. Mater. Chem. B*, 2014, **2**, 1653.
27. Y. H. Deng, D. W. Qi, C. H. Deng, X. M. Zhang, and D. Y. Zhao, *J. Am. Chem. Soc.*, 2008, **130**, 28.
28. J. F. Zeng, L. H. Jing, Y. Hou, M. X. Jiao, R. R. Qiao, Q. J. Jia, C. Y. Liu, F. Fang, H. Lei, and M. Y. Gao, *Adv. Mater.*, 2014, **26**, 2694.
29. S. Y. Gao, Y. G. Shi, S. X. Zhang, K. Jiang, S. X. Yang, Z. D. Li, and E. Takayama-Muromachi, *J. Phys. Chem. C*, 2008, **112**, 10398.
30. X. Liu, X. Chen, Y. F. Li, X. Y. Wang, X. M. Peng, and W. W. Zhu, *ACS Appl. Mater. Interfaces*, 2012, **4**, 5169.
31. E. A. Osborne, T. M. Atkins, D. A. Gilbert, S. M. Kauzlarich1, K. Liu, and A. Y. Louie, *Nanotechnology*, 2012, **23**, 215602.
32. X. Y. Lu, M. Niu, R. R. Qiao, and M. Y. Gao, *J. Phys. Chem. B*, 2008, **112**, 14390.
33. M. E. Khosroshahi, and L. Ghazanfari, *J. Magn. Magn. Mater.*, 2012, **324**, 4143.
34. B. B. Nathwani, M. Jaffari, A. R. Juriani, A. B. Mathur, and K. E. Meissner, *IEEE T Nanobiosci.*, 2009, **8**, 72.
35. X. Fei, Z. Z. Shao, and X. Chen, *J. Mater. Chem. B*, 2013, **1**, 213.
36. Y. G. Chung, K. Algarrahi, D. Franck, D. D. Tu, R. M. Adam, D. L. Kaplan, C. R. E. Jr., and J. R. Mauney, *Biomaterials*, 2014, **35**, 7452.
37. E. Wenk, A. J. Wandrey, H. P. Merkle, and L. Meinel, *J. Controlled Release*, 2008, **132**, 26.
38. F. P. Seib, E. M. Pritchard, and D. L. Kaplan, *Adv. Funct. Mater.*, 2013, **23**, 58.
39. N. C. Tansil, L. D. Koh, and M. Y. Han, *Adv. Mater.*, 2012, **24**, 1388.
40. D. H. Kim, Y. S. Kim, J. Amsden, B. Panilaitis, D. L. Kaplan, F. G. Omenetto, M. R. Zakin, and J. A. Rogers, *Appl. Phys. Lett.*, 2009, **95**, 133701.
41. P. Domachuk, K. Tsioris, F. G. Omenetto, and D. L. Kaplan, *Adv.Mater.*, 2010, **22**, 249.
42. F. G. Omenetto, and D. L. Kaplan, *Nat. Photon.*, 2008, **2**, 641.
43. X. Fei, Z. Z. Shao, and X. Chen, *Nanoscale*, 2013, **5**, 7991.
44. X. Fei, M. H. Jia, X. Du, Y. H. Yang, R. Zhang, Z. Z. Shao, X. Zhao, and X. Chen, *Biomacromolecules*, 2013, **14**, 4483.
45. S. J. Xu, L. Yong, and P. Y. Wu, *Appl. Mater. Interfaces*, 2013, **5**, 654.
46. M. Deng, Z. B. Huang, Y. W. Zou, G. F. Yin, J. Liu, and J. W. Gu. *Colloids Surf., B*, 2014, **116**, 465.
47. Q. Lu, X. L. Wang, S. Z. Lu, M. Z. Li, D. L. Kaplan, and H. S. Zhu, *Biomaterials*, 2011, **32**, 1059.
48. H. Deng, X. L. Li, Q. Peng, X. Wang, J. P. Chen, and Y. D. Li, *Angew. Chem., Int. Ed.*, 2005, **44**, 2782.

Journal of Materials Chemistry B Accepted Manuscript

This journal is © The Royal Society of Chemistry [year]

49. J. E. Frith, D. J. Menzies, A. R. Cameron, P. Ghosh, D. L. Whitehead, S. Gronthos, A. C. W. Zannettino, and J. J. Copper-White, *Biomaterials*, 2014, **35**,1150.

50. X. Q. Wang, and D. L. Kaplan, *Macromol. Biosci.*, 2011, **11**, 100.

51. R. N. Muller, P. Gillis, F. Moiny, and A. Roch, *Magn. Reson. Med.*, 1991, **22**, 178.

52. A. Bjørnerud, and L. Johansson, *NMR Biomed.*, 2004, **17**, 465.

53. S. M. Bai, S. S. Liu, C. C. Zhang, W. Xu, Q. Lu, H. Han, D. L. Kaplan, and H. S. Zhu, *Acta Biomaterialia*, 2013, **9**, 7806.

54. S. H. Xuan, F. Wang, J. M. Y. Lai, K. W. Y. Sham, Y. X. J. Wang, S. F. Lee, J. C. Yu, C. H. K. Cheng, and K. C. F. Leung, *ACS Appl. Mater. Interfaces*, 2011, **3**, 237.

55. S. H. Xuan, F. Wang, Y. H. J. Wang, J. C. Yu, and K. C. F. Leung, *J. Mater. Chem.*, 2010, **20**, 5086.

56. K. X. Yao, and H. C. Zeng, *J. Phys. Chem. C*, 2007, **111**, 13301.

57. T. He, D. R. Chen, and X. L. Jiao, *Chem. Mater.*, 2004, **16**, 737.

58. Y. F. Ma, Q. L. Feng, and X. Bourrat, *Mater. Sci. Eng. C*, 2013, **33**, 2413.

59. X. L. Zhang, Z. H. Fan, Q. Lu, Y. L. Huang, D.L. Kaplan, and H. S. Zhu, *Acta Biomater.*, 2013, **9**, 6974.

60. B. B. Peksen, C. Uzelakcil, A. Gunes, O. Malay, and O. Bayraktar, *J. Chem. Technol. Biotechnol.*, 2006, **81**, 1218.

61. X. H. Lin, G. B. Ji, Y. S. Liu, Q. H. Huang, Z. H. Yang, and Y. W. Du, *CrystEngComm.*, 2012, **14**, 8658.

62. Q. Song and Z. J. Zhang, *J. Am. Chem. Soc.*, 2004, **126**, 6164.

Journal of Materials Chemistry B Accepted Manuscript

Figure 1 SEM images of the products prepared under different silk fibroin contents. 10 ml of silk fibroin aqueous solutions added into the reaction system had different concentrations as follows: (a) pure water, (b) 0.1wt%, (c) 2.0 wt%, (d) 4.0 wt%, (e)7.0 wt%, (f)10.0 wt%, (g)15.0 wt%

Figure 2 TEM images of the products prepared under different silk fibroin contents. 10 ml of silk fibroin aqueous solutions added into the reaction system had different concentrations as follows: (a) pure water, (b) 0.1 wt%, (c) 2.0 wt%, (d) 4.0 wt%, (e)7.0 wt%, (f)10.0 wt%, (g)15.0 wt%.

Figure 3 XRD patterns of Fe_3O_4/SF nanomaterial prepared under different silk fibroin contents. 10 ml of silk fibroin aqueous solutions added into the reaction system had different concentrations as follows: (a) pure water, (b) 0.1 wt%, (c) 2.0 wt%, (d) 4.0 wt%, (e)7.0 wt%, (f)10.0 wt%, (g)15.0 wt%.

Figure 4 (a) Magnetic hysteresis loops of Fe_3O_4/SF and Fe_3O_4 nanoparticles measured at room temperature by VSM, Inserts were the photographs of Fe_3O_4/SF suspension and Fe_3O_4/SF with an external magnetic field, (b) T_2-weighted MRI image of Fe_3O_4/SF in aqueous solution (containing 1% agarose) with different Fe concentrations, (c) The linear fitting of relaxation rates (R_2) versus Fe concentrations of Fe_3O_4/SF. Additionally, R_2 is equal to 1/ T_2, and the relaxivity value (r_2) was obtained from the slopes of the line.

Figure 5 Relative viabilities of Hs 865.sk cells (a) and NCI-H460 cells (b) determined by the CCK8 assay after incubation with Fe_3O_4/SF and Fe_3O_4 nanoparticles with different Fe concentrations at 37 ^oC for 24h. The cells cultured in same culture medium without Fe as positive control. Cell viability in eight parallel wells was evaluated for each dose, and each experiment was repeated at least three times. *Statistically significant $P<0.05$.

Figure 6 Linkage of biotinylated anti-CD_3 antibody to the surface of FITC-Avidin-Fe_3O_4/SF and specific targeting of the modified Fe_3O_4/SF to CD_3 positive T-lymphocytic cell line Jurkat. (a, b): positive groups (CD_3 + lymphocytes); (c, d) negative groups (human bone marrow-derived mescenchymal stem cells). (a, c): the overlay of DAPI fluorescence, FITC fluorescence and the bright field images of cells (the DAPI fluorescence associated with nucleus, and the FITC fluorescence associated with Biotinylated anti-CD_3 antibody-FITC-Avidin-Fe_3O_4/SF); (b, d) the bright field images of cells.

Scheme 1 Possible formation mechanism of Fe_3O_4/SF nanomaterial.

Journal of Materials Chemistry B Accepted Manuscript

This journal is © The Royal Society of Chemistry [year]

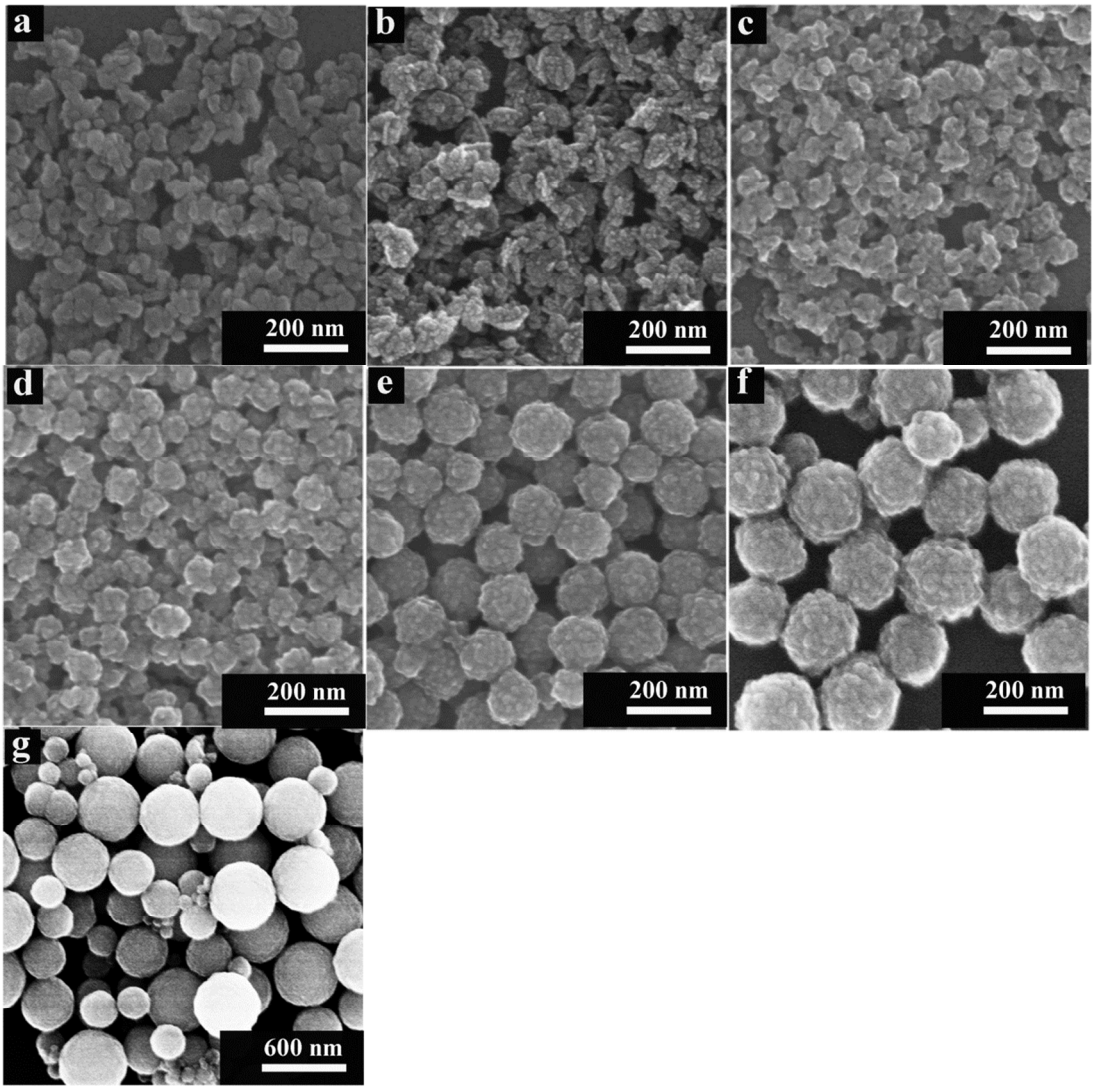

Figure 1

Journal of Materials Chemistry B Accepted Manuscript

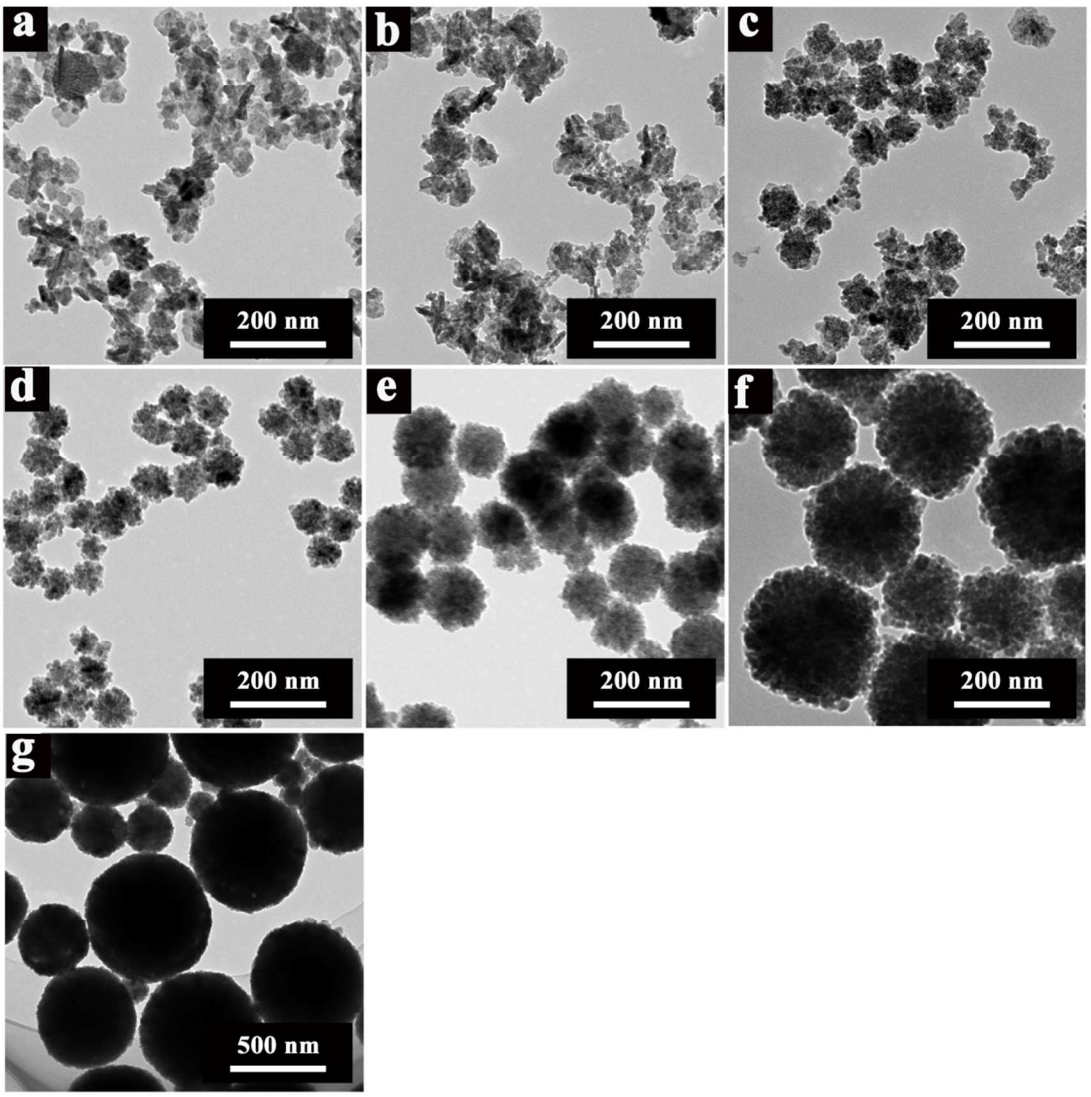

Figure 2

Journal of Materials Chemistry B Accepted Manuscript

This journal is © The Royal Society of Chemistry [year]

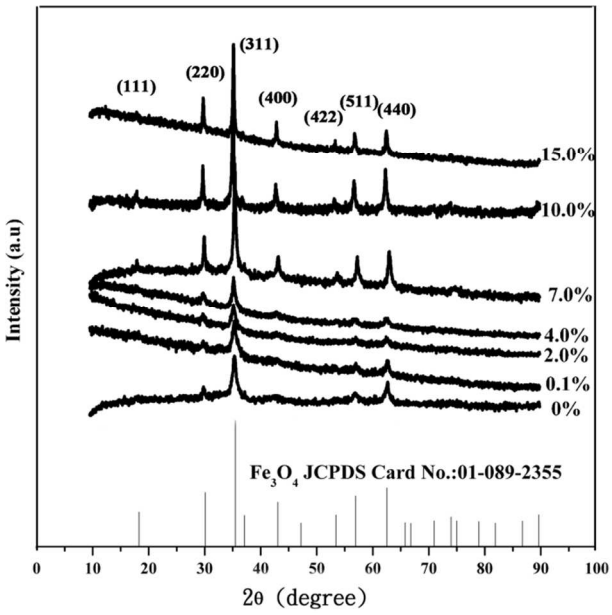

Figure 3

Journal of Materials Chemistry B Accepted Manuscript

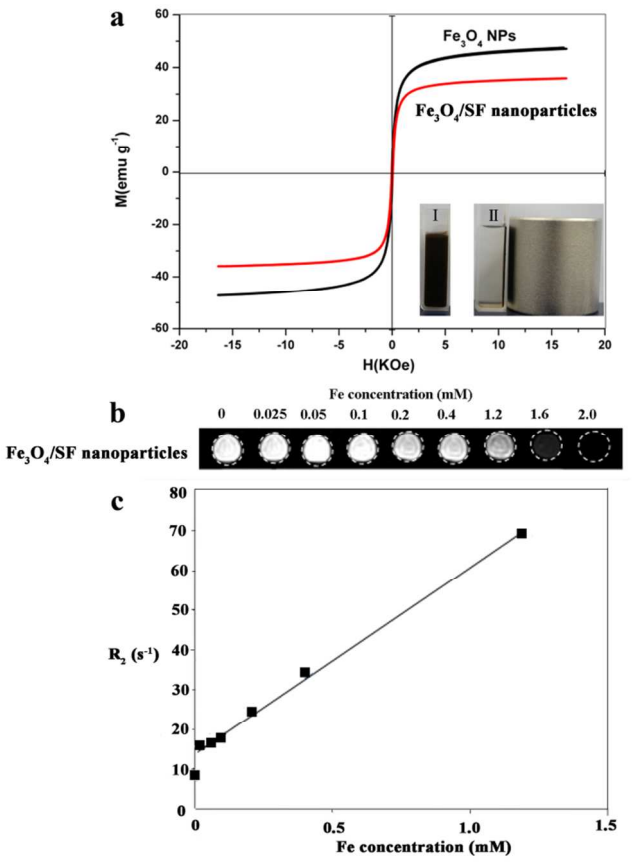

Figure 4

Journal of Materials Chemistry B Accepted Manuscript

This journal is © The Royal Society of Chemistry [year]

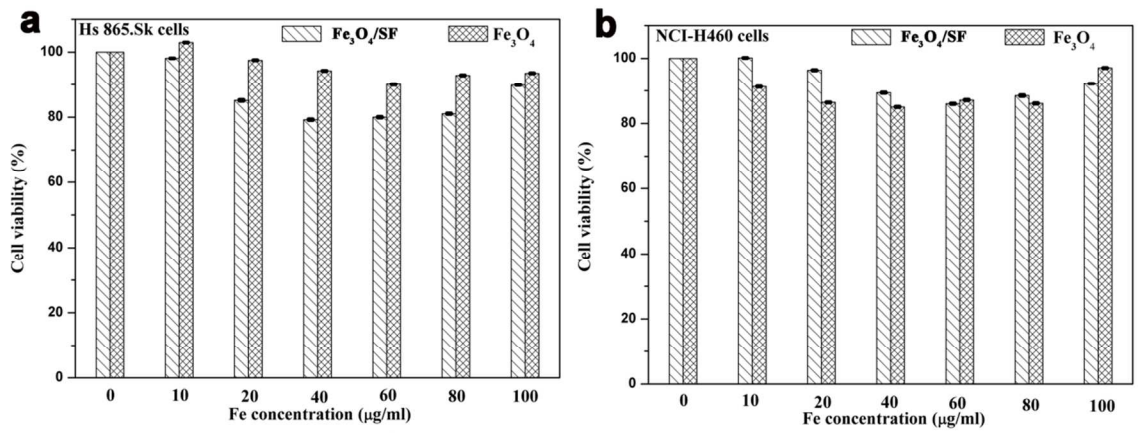

Figure 5

Journal of Materials Chemistry B Accepted Manuscript

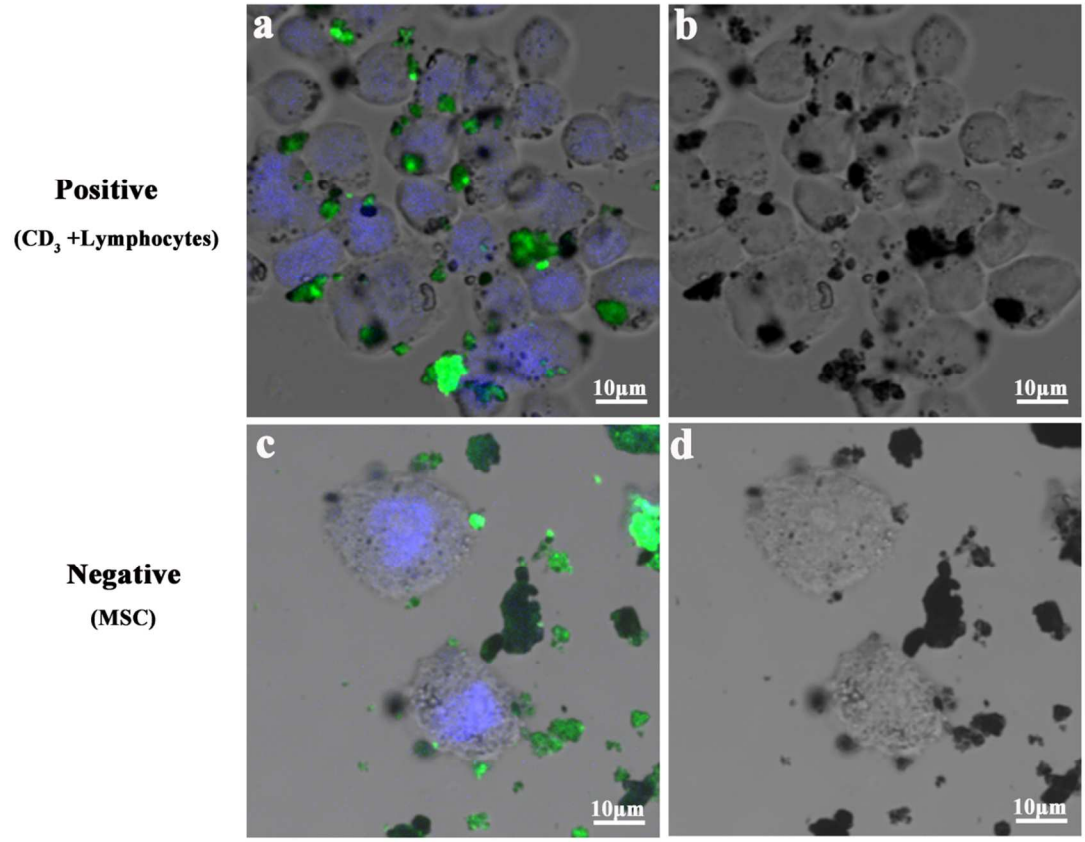

Figure 6

Journal of Materials Chemistry B Accepted Manuscript

This journal is © The Royal Society of Chemistry [year]

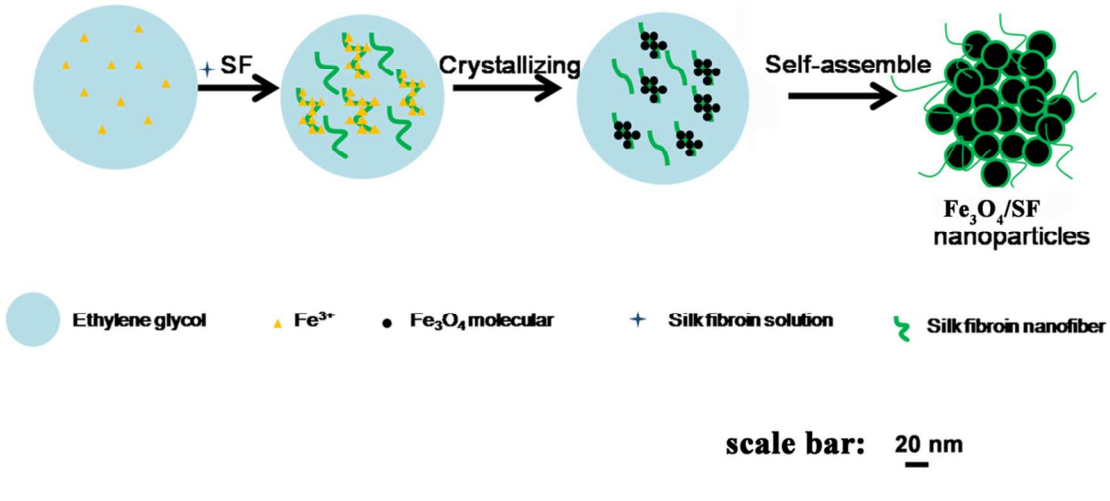

Scheme 1

Journal of Materials Chemistry B Accepted Manuscript